

# Gross Error Detection and Data Correction in IIoT-Based Data Center Cooling System

Abdul Hamid<sup>1</sup>, Eko Mursito Budi<sup>2</sup>, Estiyanti Ekawati<sup>2</sup>

<sup>1</sup> Instrumentation and Control Engineering, Institut Teknologi Bandung, Bandung, Indonesia

<sup>2</sup> Engineering Physics, Institut Teknologi Bandung, Bandung, Indonesia  
hamidabdul776@outlook.co.id

Accepted on 26 June 2024

Approved on 09 July 2024

**Abstract**— A data center always require a proper cooling system. This research study a data center with water based cooling system that consists of two chillers and two in-rack coolers. To control the system, an Industrial Internet of Things (IIoT) infrastructures has been deployed. It able to monitors real-time data from various sensors such as temperature (T), pressure (P), water flow (Q). The data were supposed to be used for optimization. However, early assessment showed that there were discrepancies between the sensors. Therefore, the data reconciliation method is very important to get valid data from the sensor by utilizing the least square optimization problem method. obtained the results of error detection on the temperature sensor reading +/- 2.5 degrees with an accuracy of 3 numbers behind the comma, then analyzed the Mean Square Error and Mean Average Error at the time before reconciliation the results were 7.21 and 2.68, and after the reconciliation process and gross error obtained the results of Mean Square Error of 0.33 and Mean Average Error of 0.5 from these results it can be concluded that the reconciliation and gross error detection method used with the least square method is better than the gross error detection method.

**Index Terms**— Colleration matrix; Gross error detection; Industrial Internet of things; Least-square optimization method.

## I. INTRODUCTION

The advent of Industry 4.0 has ushered in a paradigm shift across diverse industrial sectors, necessitating the ubiquitous integration of data centers. Industry 4.0, a convergence of digital and physical technologies in industrial processes, has precipitated an escalating demand for High-Performance Computing (HPC). In this landscape, cloud technology services and the imperative for high computing loads constitute pivotal facets in industrial operations, facilitating real-time data processing, analysis, and responsiveness. Data centers, as linchpins in efficient data storage and management, furnish the computational prowess requisite for expanse data analytics [1].

Nevertheless, the challenges intrinsic to high computing loads in the industry 4.0 milieu exert formidable stress on data center performance. This necessitates the capacity to adeptly manage voluminous

data and promptly respond to exigent demands [2]. Operational challenges further manifest in the inefficiencies of water-cooling systems, characterized by excessive energy consumption and necessitating disruptive downtimes for maintenance [3]. The utilization of data reconciliation methods becomes imperative to verify the accuracy of every sensor employed in process control [4] to archive goal creation an optimal control system and can reduce time of the cooling machine. other challenging in data center systems revolves around maintaining room temperatures below the dew point, crucial for optimal functionality of computer servers within the data center environment [5].

Therefore, we are developing an IIoT system for the water-based cooling machine in the data center, which will be constructed in Labtek 6, Building of Engineering Physics, Faculty of Industrial Technology, Institute Teknologi Bandung. One of the key aspects we need to focus on is ensuring that the measurement data are accurate to make the process effective and efficient [6]. Building an IIoT Integration system, measurement error can sometimes occur, and this error can be categorized into random errors and gross error [7]. These errors need to be minimized during the data acquisition process to make sure all those data for acquisition were accurate [8]. One or other method can be use is to minimize the objective function in linear state space equation over time and by detecting gross errors through a physical quantity approach in the control process has been used [9].

The approach involves employing the SciPy optimization method to minimize the objective function using a general equation for Least Square Optimization. The input for the SciPy function includes a correlation matrix, and the relationships between various processes in the data center cooling system are visualized using a heatmap method. Prior to analysis, the dataset undergoes preprocessing, which includes noise detection, training on 80% of the data, and validation using the remaining 20%. The primary goal of this process is to identify measurement errors in the sensors and subsequently adjust the measured values.

II. METHODS

A. Research Objective

The research focuses on a data center with water based cooling system located at Labtek 6, Engineering Physics, Faculty of Industrial Technology, Bandung Institute of Technology. An IIoT system for this system has been developed using the Node-RED platform. During the implementation of the IIoT integration system, it was observed that some sensors were less accurate, necessitating a gross error detection and correction method in the data acquisition process. This research involves several stages, as depicted in the overall research flow chart in Fig. 1.

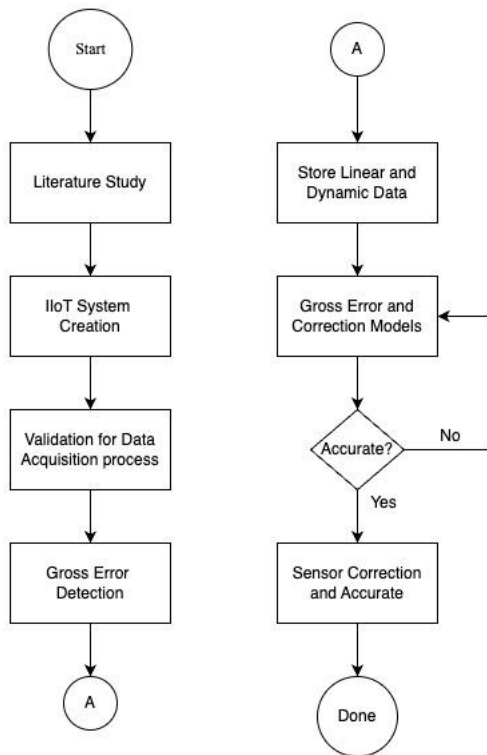


Fig. 1. Research Flow Diagram

B. Water Based Cooling System & Instrumentation

The schematic design of the Piping & Instrument Diagram in this study, as illustrated in Fig.2 reveals the representation of Chiller 1 and Chiller 2 as CH.1 and CH.2, both sharing the same water flow. A mixing pipe serves as a blending and redundancy system, enabling the alternating activation or deactivation of Chiller 1 and Chiller 2 every 12 hours. The sequence begins with Chiller 1 powered by Motor 1 (CHWP 1) followed by Chiller 2 powered by Motor 2 (CHWP 2). The controller employed in this study is a PLC of CP2E type, specifically designed for reading and controlling the data center cooling system effectively.

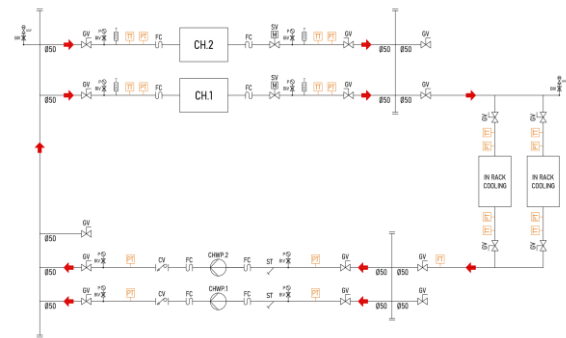


Fig. 2. Piping and Instrument Diagram

In the section illustrating the water inlet represented by red arrows from Chiller 1 and 2 before entering the Mixing Pipe, Solenoid Valves (SV) are strategically placed in each chiller section. This is to ensure that the water flow is directed only to the active chiller while the inactive one remains unaffected. After entering the mixing pipe, water flow is propelled by a pump towards the In-rack Cooling section through a branching pipe system, ensuring even distribution. Temperature (TT) and pressure (PT) sensors are strategically placed at the entry and exit points of the In-rack Cooling system. Each pipe in this process is equipped with temperature and pressure sensors to analyze the temperature and pressure differences between the incoming and outgoing water from Chiller 1 and Chiller 2. Additionally, a flow sensor (FT) is installed to detect any water leakage within the system. This P&ID system constructed fulfills the criteria for conducting data correction and detecting gross error values effectively. Multiple sensors installed in each relevant process enable the application of reconciliation principles for accurate data correction, ensuring high precision and suitability [18].

C. IIoT System

The architectural system for IoT integration in Data Center cooling machines utilizes the Node-RED platform. It serves as a communication bridge between physical devices (OT) and the IT system, allowing every process on the machine to be automatically recorded in a MySQL database and displayed on the HMI panel, as shown in Fig 3.

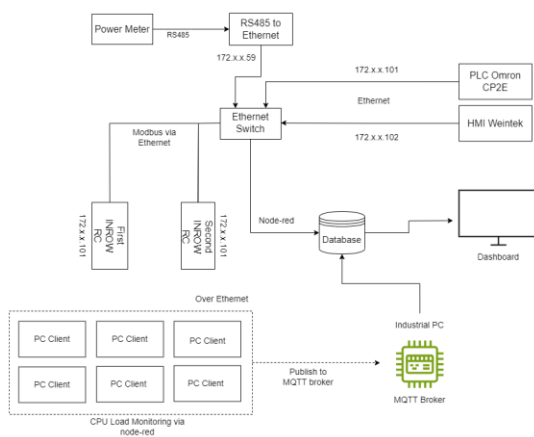


Fig. 3. IT Diagram for IT Process

Furthermore, Fig.4 illustrates the configuration of OT devices, which consist of sensors and actuators controlled by an Omron CP2E N-30DRA PLC. This PLC is connected via Analogue, Digital, or RS485 communication pin and the developed system must ensure that the data acquisition process and the implemented control system operate smoothly and without interruptions.

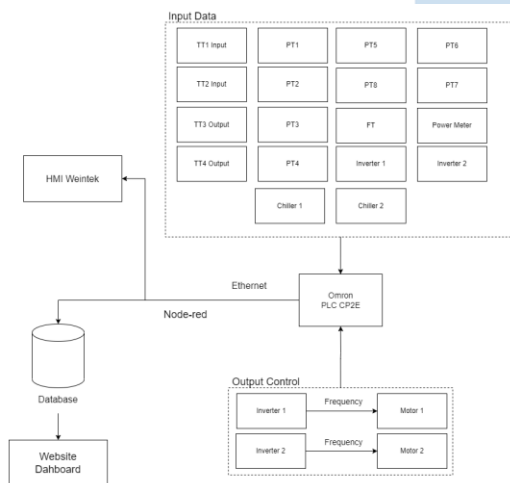


Fig. 4. OT Diagram for Field Device

#### D. Gross Error Detection & Correction Model

In state space analysis, a model is typically represented by first-order differential equations in a steady-state system [13]. The general state space equation is expressed as follows:

$$\dot{x}(t) = Ax(t) + Bu(t) \quad (1)$$

$$y(t) = Cx(t) + Du(t) \quad (2)$$

Equation (1) represents the state space equation, and equation (2) is the output equation of a linear system [14]. The author employs the Least Squares Optimization method to find the minimum value of the objective function in a linear system. This method is preferred over Weighted Least Squares because the

dataset is predominantly linear, as described by the general function in Equation (3).

$$\min \sum_{i=1}^n \omega_i (x_i - \hat{x}_i)^2 \quad (3)$$

And referring to Equation (1), we get Equation (4) matrix notation.

$$\min(x - \hat{x})^T W(x - \hat{x}) \quad (4)$$

To solve the optimization problem, the method of Lagrange multipliers, as shown in Equation (5), is used. This approach involves obtaining the value of the partial derivative of the Lagrangian function ( $\mathcal{L}$ ) with respect to  $x$  dan  $\lambda$  by setting the equation equal to zero [15]. The optimal result of data reconciliation ( $X_r$ ) and the offset/bias value, which are necessary for data correction, are then determined. These results represent the accuracy of a sensor under steady-state conditions.

$$\mathcal{L}_{(x,\lambda)} = (x - \hat{x})^T W(x - \hat{x}) + \lambda^T (A_x + b) \quad (5)$$

In a control process, an essential variable for data processing is converting time-based state space equations to discrete-based state space equations. This conversion requires selecting an appropriate sampling rate to accurately model a continuous system as a discrete one [16]. To minimize errors resulting from the discretization of the state space, suitable sampling intervals are necessary, these intervals are typically as small as possible relative to the system time constant, or the real-time sampling frequency of data obtained from the control process. The discrete state space equations are represented by Equation (6) and Equation (7) as follows:

$$X_k = FX_{k-1} + GU_{k-1} + W_k \quad (6)$$

$$Y_k = HX_k + V_k \quad (7)$$

Then, the data bias parameters represented by  $W_k V_k$  and errors can be shown in Equation (8) as follows:

$$E[W_k] = E[V_k] = 0$$

$$Cov[W_k] = Q$$

$$Cov[V_k] = R$$

$$Cov[W_k, W_i] = Cov[V_k, V_j] = 0$$

$$Cov[W_k, V_j] = 0$$

The equation aims to ensure that the expected values of  $W_k$  and  $V_k$  are zero, with their covariances being  $Q$  and  $R$  respectively.

#### E. Gross Error Detection & Correction Calculation

The process of gross error detection and data correction in a system involves collecting real-time sensor data and comparing readings from potentially erroneous sensors with those from accurate sensors.

while adhering to relevant physical laws. Corrected sensors must maintain a constant physical mass and be within a relatively close range.

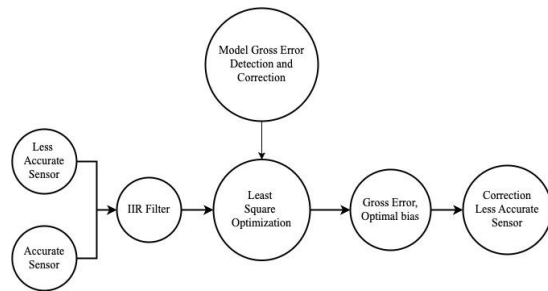


Fig. 5. Gross Error detection and Correction process

Figure 5 shows the data flow diagram of error detection and correction process. It begins by reading the data from the accurate sensors as well as the less accurate ones. To reduce the noise, the data then filtered with an IIR filter [10]. This is followed by sampling the steady state of the data center cooling process, indicated by water temperature measurements that match the setpoint. If the system is functioning normally but missing data is detected, the random forest method is used to predict and fill in the missing values [11]. Then, to analyze the processes and their correlations, resulting in a correlation matrix. Heatmap analysis is used to identify and visualize the relationships between each process within the system [12]. The resulting correlation matrix will be used as an input data for gross error detection.

In employing the least square optimization method, the dataset used must be in a stable state. This requirement arises because the least square optimization method necessitates stable data to accurately minimize objective functions. One critical factor affecting the accuracy of the least square optimization model is ensuring that both the training and validation data are free from noise. Therefore, it is essential to preprocess the data to eliminate any noise and enhance the reliability of the optimization results digital filter need to be applying on training and validation data. On this research specifically use an IIR filter, to the obtained dataset to eliminate noise in the sensor reading system. This results in a noise-free set of sensor data, aiming to provide the most optimal correction results. Following this, a heatmap analysis is performed on the filtered dataset to determine the correlation between the various processes.

The resulting matrix is then used as input data to minimize the objective function using the least square optimization method. Once the objective function is derived, it yields the bias value ( $b$ ), which is subsequently used to correct data from sensors exhibiting intolerable bias [17]. Then, to correct the sensor data using Equation (9) to achieve accurate data readings.

$$\Delta_{correction} = (Xr - b) - E_{data} \quad (9)$$

After obtaining the corrected data values from the validation process of the sensor readings, the Mean Square Error (MSE) and Mean Absolute Error (MAE) were evaluated. The errors were assessed for the corrected sensor data in comparison to the calibrated sensor data. If the MSE and MAE values for the corrected sensor data are within  $\pm 0.5\%$  of the calibrated sensor data, it can be concluded that the applied method is successful. This indicates that the corrections have effectively improved the accuracy of the sensor readings.

### III. RESULTS AND DISCUSSION

#### A. IIoT data logging

The data logger used in this research samples data every 10 seconds for all processes occurring within the water-based data center cooling machine and some crucial sensors are read with a per-second sampling rate, including the temperature sensor in the pipe (TT), the pressure sensor in the pipe (PT), the water flow sensor at the chiller output (FT1), and the water flow sensor at the chiller return (FT2). Fig. 8 shows the temperature sensor data readings with a 10-second time sampling interval. The set point changes sequentially from 16 degrees to 18 degrees, and then to 20 degrees, resulting in the graph shown in Fig 6.

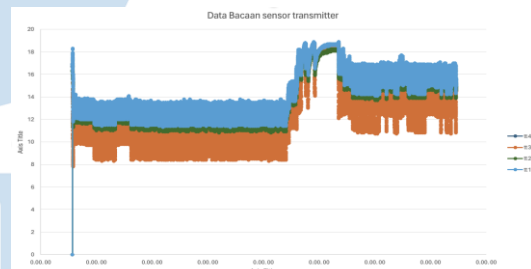


Fig. 6. Data Logger within 10 second sampling time

#### B. Error Detection & Correction Model

Based on the development of the IIoT system for data center cooling machines, sensors were positioned according to the P&ID design drawing. The system schematic is depicted in Fig. 7.

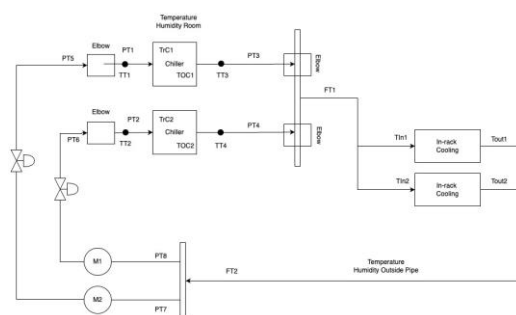


Fig. 7. Schematic of the IoT system of Water-based Data Center Cooling Machine

The sensor placement illustrated in Fig 7 adheres to the previously designed P&ID. Temperature (TT) and pressure (PT) sensors have been installed at the mixing pipe outlets (ToC) and returns (TrC) of the cooling machine. The water flow is monitored both before and after the in-rack cooling process to evaluate for potential leaks in the closed-loop system. This can be represented in the physical model as follows:

$$\begin{aligned}
 TrC1 - TT1 &= 0 \text{ and } TrC2 - TT2 = 0 \\
 ToC1 - TT3 &= 0 \text{ and } ToC2 - TT4 = 0 \\
 PT1 + \hat{x} &= PT5 \text{ and } PT2 + \hat{x} = PT6 \\
 PT1 + \hat{x} &= PT3 \text{ and } PT2 + \hat{x} = PT4 \\
 PT5 + \hat{x} &= PT7 \text{ and } PT6 + \hat{x} = PT8 \\
 Tin1 &= TT3 - \hat{x} \text{ and } Tin2 = TT4 - \hat{x} \\
 Tout2 &= Tin1 - \hat{x} \text{ and } Tout1 = Tin1 - x \\
 FT1 &= FT2 = FT3 = FT4
 \end{aligned} \quad (10)$$

In this model, it is assumed that the water flow rate remains constant and is independent of any processes occurring within the system. Therefore, it can be represented in matrix form as follows:

1. Current model condition  $TrC1 - TT1 = 0$  and  $TrC2 - TT2 = 0$ .

$$\begin{bmatrix} TT_1 \\ TT_2 \\ TrC_1 \\ TrC_2 \end{bmatrix} = \begin{bmatrix} -1 & 0 & 1 & 0 \\ 0 & -1 & 0 & 1 \\ 1 & 0 & -1 & 0 \\ 0 & -1 & 0 & 1 \end{bmatrix} \begin{bmatrix} TT_1 \\ TT_2 \\ TrC_1 \\ TrC_2 \end{bmatrix} + b \quad (11)$$

2. Current model condition  $ToC1 - TT3 = 0$  and  $ToC2 - TT4 = 0$ .

$$\begin{bmatrix} TT_3 \\ TT_4 \\ ToC_1 \\ ToC_2 \end{bmatrix} = \begin{bmatrix} -1 & 0 & 1 & 0 \\ 0 & -1 & 0 & 1 \\ -1 & 0 & 1 & 0 \\ 0 & -1 & 0 & 1 \end{bmatrix} \begin{bmatrix} TT_3 \\ TT_4 \\ ToC_1 \\ ToC_2 \end{bmatrix} + b \quad (12)$$

3. Current model condition  $PT1 + \hat{x} = PT5$  and  $PT2 + \hat{x} = PT6$ .

$$\begin{bmatrix} PT_1 \\ PT_2 \\ PT_5 \\ PT_6 \end{bmatrix} = \begin{bmatrix} 1 & 0 & -1 & 0 \\ 0 & 1 & 0 & -1 \\ 1 & 0 & -1 & 0 \\ 0 & 1 & 0 & -1 \end{bmatrix} \begin{bmatrix} PT_1 \\ PT_2 \\ PT_5 \\ PT_6 \end{bmatrix} + b \quad (13)$$

4. Current model condition  $PT1 + \hat{x} = PT3$  and  $PT2 + \hat{x} = PT4$ .

$$\begin{bmatrix} PT_1 \\ PT_2 \\ PT_5 \\ PT_6 \end{bmatrix} = \begin{bmatrix} 1 & 0 & -1 & 0 \\ 0 & 1 & 0 & -1 \\ 1 & 0 & -1 & 0 \\ 0 & 1 & 0 & -1 \end{bmatrix} \begin{bmatrix} PT_1 \\ PT_2 \\ PT_5 \\ PT_6 \end{bmatrix} + b \quad (14)$$

5. Current model condition  $PT5 + \hat{x} = PT7$  and  $PT6 + \hat{x} = PT8$ .

$$\begin{bmatrix} PT_5 \\ PT_6 \\ PT_7 \\ PT_8 \end{bmatrix} = \begin{bmatrix} 1 & 0 & -1 & 0 \\ 0 & 1 & 0 & -1 \\ -1 & 0 & 1 & 0 \\ 0 & -1 & 0 & 1 \end{bmatrix} \begin{bmatrix} PT_5 \\ PT_6 \\ PT_7 \\ PT_8 \end{bmatrix} + b \quad (15)$$

6. Current model condition  $Tin1 = TT3 - \hat{x}$  and  $Tin2 = TT4 - \hat{x}$ .

$$\begin{bmatrix} TT_3 \\ TT_4 \\ Tin_1 \\ Tin_2 \end{bmatrix} = \begin{bmatrix} 1 & 1 & -1 & 0 \\ 1 & 1 & -1 & -1 \\ 1 & 1 & -1 & 0 \\ 1 & 1 & 0 & -1 \end{bmatrix} \begin{bmatrix} TT_3 \\ TT_4 \\ Tin_1 \\ Tin_2 \end{bmatrix} + b \quad (16)$$

7. Current model condition  $Tout2 = Tin1 - \hat{x}$  and  $Tout1 = Tin1 - x$ .

$$\begin{bmatrix} Tin_1 \\ Tin_2 \\ Tout_1 \\ Tout_2 \end{bmatrix} = \begin{bmatrix} 1 & 0 & -1 & 0 \\ 0 & 1 & 0 & -1 \\ 1 & 0 & -1 & 0 \\ 0 & 1 & 0 & -1 \end{bmatrix} \begin{bmatrix} Tin_1 \\ Tin_2 \\ Tout_1 \\ Tout_2 \end{bmatrix} + b \quad (17)$$

8. Current model condition  $FT1 = FT2 = FT3 = FT4$ .

$$\begin{bmatrix} FT_1 \\ FT_2 \\ FT_3 \\ FT_4 \end{bmatrix} = \begin{bmatrix} 1 & 1 & 1 & 1 \\ 1 & 1 & 1 & 1 \\ 1 & 1 & 1 & 1 \\ 1 & 1 & 1 & 1 \end{bmatrix} \begin{bmatrix} FT_1 \\ FT_2 \\ FT_3 \\ FT_4 \end{bmatrix} + b \quad (18)$$

### C. Data Processing

The initial step involved analyzing the system by distinguishing between transient and steady-state conditions. After separating the transient and steady-state data, noise was detected in the data. Therefore, a digital filter was required to remove the noise. An Infinite Impulse Response (IIR) filter was employed for this purpose. The IIR filter was chosen to mitigate overfitting and underfitting, ensuring clean data for machine learning applications, which results in high accuracy. Assuming a fourth-order IIR filter with a cutoff value of 10, the filtered data, as shown in Figure 10 was the reduces noise in the dataset.

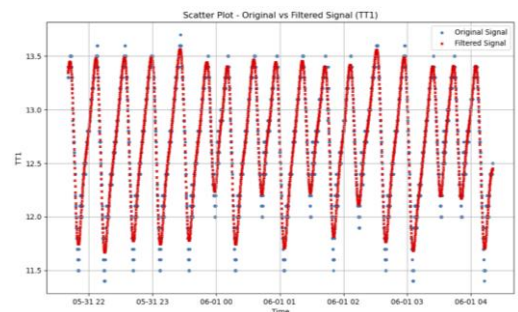


Fig. 8. Plot data from original data comparing with filtered data

The subsequent step involves constructing matrix A, which represents the correlation matrix derived from the least squares optimization problem to determine the objective function. This process utilizes a heat-map analysis approach based on the derived physical equations, as depicted in Fig. 11. Higher values in the heat-map, the 1 value in result that

indicate strong relationships between the conditions being analyzed.

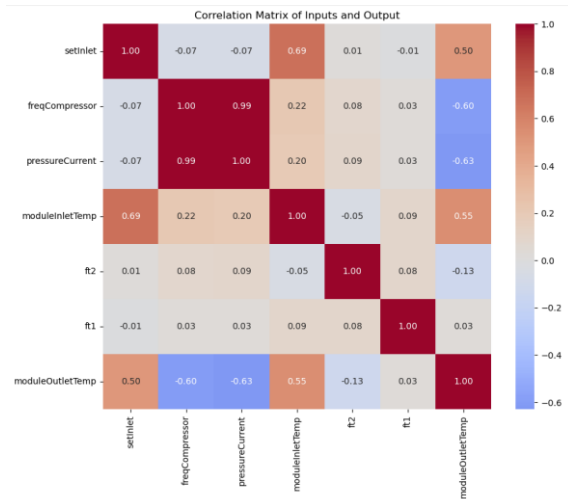


Fig. 9. Result of correlation matrix analysis using heat-map method

Subsequently, from these results, the author derived a 24x24 correlation matrix equation. Substituting this matrix equation into the least squares optimization method yielded  $X_r$  values, representing the accuracy of sensor readings, and optimal bias values ( $b$ ) for each sensor. The optimal values of  $X_r$  and  $b$  obtained sequentially for the temperature sensor in the pipe (TT) and the water flow rate sensor (FT) readings are as follows:

1. Temperature sensor (TT)  
 Optimal  $X_r = [12.69 \ 12.36 \ 11.52 \ 12.48]$   
 Optimal  $b = [-2.5 \ -2.57 \ 1.42 \ 1.43]$

This represents sensor condition TT1, TT2, TT3, TT4 that located on pipping area in return and outlet Chiller.

2. Water Flow Sensor (FT)  
 Optimal  $X_r = [23.42 \ 12.40 \ 17.21 \ 9.84]$   
 Optimal  $b = [-6.28 \ -6.28 \ -6.28 \ -6.28]$

This represents sensor condition FT1, FT2, FT3, FT4 that located on return, outlet chiller, inside in rack-cooling, and feedback from in rack-cooling.

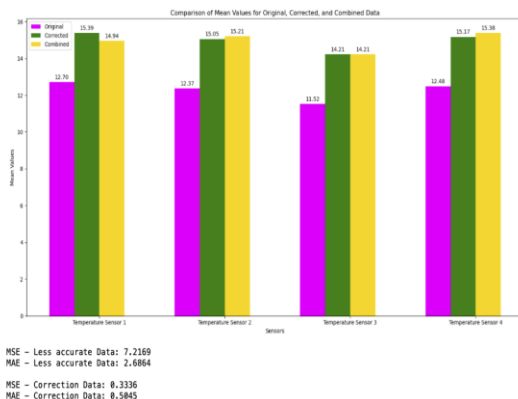


Fig. 10. Graphic plot result for temperature data correction

Then, after getting the results of the optimal  $X_r$  and optimal  $b$  values. Next, to make corrections, the sensor data is obtained using Equation (9). and the results obtained are as in Figure 10, namely a graphic plot of the results of the corrected temperature sensor data readings compared to the calibrated temperature sensor. The graph indicates a good adjustment with MAE results of 0.5045 and MSE 0.335.

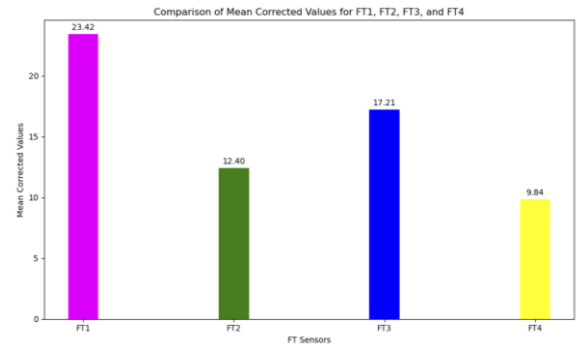


Fig. 11. Graph comparison on Water Flow sensor

The next analysis is the water flow sensor, the results obtained as in Figure 10 show a graph of the relationship between the water flow sensor before and after data correction and compared with the sensor that is considered accurate. On Pressure sensor there is no problem with that condition. everything was accurate and no need adjustment variable.

#### IV. CONCLUSION

In the conducted research, it was determined that the number of sensors utilized in the data center cooling machine meets the criteria for detecting gross errors and correcting sensor inaccuracies. This enables thorough analysis and correction of inaccurate sensor readings to achieve high accuracy.

From the error correction process of sensor reading data compared to the original data, the results showed an MSE of 7.216 and an MAE of 2.6864. Furthermore, when comparing the error-corrected sensor reading data to the accurate sensor data from the water chiller machine, the results showed an MSE of 0.336 and an MAE of 0.5045.

Depending on those results of MAE and MSE obtained, it can be stated that by using the Least Square Optimization method by minimizing the objective function to obtain the gross error value and correcting the data has good performance so that this method can be applied to other data error correction case studies with a correction analysis approach on the sample dataset of steady state conditions.

#### ACKNOWLEDGMENT

This research has been part of the Laboratory Modernization Project in Engineering Physics, Faculty of Industrial Technology, ITB.

## REFERENCES

- [1] F. Ö. Koçoğlu and D. Demirkol, "Data in the Context of Industry 4.0," in *Who Runs the World: Data*, Istanbul University Press, 2020, pp. 71–92. doi: 10.26650/b/et06.2020.011.04.
- [2] M. Panarotto, O. Isaksson, and V. Vial, "Cost-efficient digital twins for design space exploration: A modular platform approach," *Comput Ind*, vol. 145, Feb. 2023, doi: 10.1016/j.compind.2022.103813.
- [3] R. He, G. Chen, C. Dong, S. Sun, and X. Shen, "Data-driven digital twin technology for optimized control in process systems," *ISA Trans*, vol. 95, pp. 221–234, Dec. 2019, doi: 10.1016/j.isatra.2019.05.011.
- [4] E. M. Budi, E. Ekawati, and B. Efendy, "Comparison of structural analysis and principle component analysis for leakage prediction on superheater in boiler," *IAES International Journal of Artificial Intelligence (IJ-AI)*, vol. 11, no. 4, p. 1439, Dec. 2022, doi: 10.11591/ijai.v11.i4.pp1439-1447.
- [5] C. F. Lazaga, A. K. S. Rodriguez, G. T. Salvador, and J.-A. V. Magsumbol, "Optimization of Dew Point, Humidity, and Temperature in Data Centers using Genetic Algorithm with Multiple Linear Regression," in *TENCON 2022 - 2022 IEEE Region 10 Conference (TENCON)*, IEEE, Nov. 2022, pp. 1–5. doi: 10.1109/TENCON55691.2022.9977710.
- [6] H. Weytjens and J. De Weerd, "Learning uncertainty with artificial neural networks for predictive process monitoring," *Appl Soft Comput*, vol. 125, p. 109134, Aug. 2022, doi: 10.1016/j.asoc.2022.109134.
- [7] A. J. Sutrisno, P. Siregar Dan, and E. Ekawati, "Program Aplikasi Rekonsiliasi Data untuk Pendeteksian Gross Error pada Sistem Tangki Ganda yang Berinteraksi," *Ktrl.Inst (J.Auto.Ctrl.Inst)*, vol. 6, no. 1, p. 2014.
- [8] S. Narasimhan and C. Jordache, "Data Reconciliation & Gross Error Detection: An Intelligent Use of Process Data," 2000.
- [9] Y. Miao, H. Su, R. Gang, and J. Chu, "Industrial Processes: Data Reconciliation and Gross Error Detection," *Measurement and Control*, vol. 42, no. 7, pp. 209–215, Sep. 2009, doi: 10.1177/002029400904200704.
- [10] S. R. Sutradhar, N. Sayadat, A. Rahman, S. Munira, A. K. M. F. Haque, and S. N. Sakib, "IIR based digital filter design and performance analysis," in *2017 2nd International Conference on Telecommunication and Networks (TEL-NET)*, IEEE, Aug. 2017, pp. 1–6. doi: 10.1109/TEL-NET.2017.8343596.
- [11] D. Borup, B. J. Christensen, N. S. Mühlbach, and M. S. Nielsen, "Targeting predictors in random forest regression," *Int J Forecast*, vol. 39, no. 2, pp. 841–868, Apr. 2023, doi: 10.1016/j.ijforecast.2022.02.010.
- [12] L. Aversano, M. L. Bernardi, M. Cimitile, M. Iammarino, D. Montano, and C. Verdone, "Using Machine Learning for early prediction of Heart Disease," in *2022 IEEE International Conference on Evolving and Adaptive Intelligent Systems (EAIS)*, IEEE, May 2022, pp. 1–8. doi: 10.1109/EAIS51927.2022.9787720.
- [13] K. Ogata, *Modern Control Engineering*. New Jersey: Pearson Education, 2010.
- [14] S. S. Rao, *Engineering Optimization: Theory and Practice*, 4th Edition., vol. 13. John Wiley & Sons, 2009.
- [15] G. Strang, *Linear Algebra and Its Applications (4th ed.)*. Brooks Cole, 2006.
- [16] K. Ogata, *Discrete Time Control Engineering*. New Jersey: Pearson Education, 2010.
- [17] W. Zhu, Z. Zhang, A. Armaou, G. Hu, S. Zhao, and S. Huang, "Dynamic data reconciliation to improve the result of controller performance assessment based on GMVC," *ISA Trans*, vol. 117, pp. 288–302, Nov. 2021, doi: 10.1016/j.isatra.2021.01.047.
- [18] J. Prakash and P. Anbumalar, "An improved recursive non-linear dynamic data reconciliation for non-linear state estimation subject to bound constraints," *Int J Adv Eng Sci Appl Math*, vol. 15, no. 1, pp. 15–23, Mar. 2023, doi: 10.1007/s12572-023-00326-7.

UMN